Theoretical and Experimental Prediction of Individual Blade Control Benefits

U.T.P. Arnold
M. Müller
P. Richter

ZF Luftfahrttechnik GmbH, Germany

Abstract

In recent years, ZF Luftfahrttechnik (ZFL) has continuously pursued the application of Individual Blade Control (IBC). Considerable experience has been accumulated in the fields of hardware design, wind tunnel and flight testing as well as in different theoretical prediction methods. In the framework of several national and international cooperation programs, ZFL is the primary hardware designer and manufacturer of complete IBC systems. This paper highlights some past and future ZFL activities in the field of IBC.

Wind tunnel test results gained in the field of rotor power reduction have been reevaluated in order to ease the transfer of wind tunnel test results to corresponding free flight cases. Test data are also evaluated with respect to the physically required actuation power which typically only amounts to a small fraction of the installed hydraulic power.

Different results in the field of vibration reduction are compared and amplitude and frequency requirements are derived. Moreover, a morphologic scheme that summarizes the data in a highly condensed form is presented. Some straightforward analytical relations are formulated which can help transfer the results to different rotor types.

Finally, some recent hardware and flight test related activities are reviewed such as dynamic and kinematic control system modeling.

Notation

A_n	HHC control amplitude of n/rev harmonic component, see equ.(1)
b	number of blades
h	distance rotor hub to c.g.
L, M	rotor hub roll, pitch moment
n	order of harmonic component
T	rotor thrust
$X = \frac{8(1-n^2)}{n\gamma}$	blade frequency-inertia parameter
$\overline{Z} = \frac{Z}{\Omega^2 S_\beta}$	normalized vertical shear force at flapping hinge
α	blade profile angle of attack
β	flapping angle
$\gamma = \frac{\rho c a R^4}{I_\beta}$	Blade LOCK number
ϑ	blade pitch control angle
μ	advance ratio
φ_n	HHC control phase angle of n/rev harmonic component, see equ. (1)
Ω	rotor angular velocity

Introduction

Theoretical and experimental investigations over a period of almost 50 years have established the notion that the extension of the conventional 1/rev blade pitch control towards higher harmonic/frequency control yields some substantial benefits in multiple aspects of the rotor performance, refs.[1] and [2]. Although most of the studies have demonstrated considerable improvements with respect to rotor induced vibrations, BVI noise radiation, blade and pitch link loads, blade motion stability, power required and high speed rotor limitations, neither Higher Harmonic Control (HHC) nor Individual Blade Control (IBC) have been implemented in a production rotorcraft and become operational until today.

Over more than ten years ZFL has pursued the development of hardware components which enable the introduction of IBC to conventional swashplate controlled rotors. A variety of different hydraulic actuators have been designed and manufactured to meet the individual requirements of wind tunnel and flight test campaigns. Beside the actuators ZFL has provided the complete hydraulic supply, the open-loop control system and all elements of the safety system. An overview of the BO-105 flight tests with the ZFL IBC system is given in ref.[4]. In 1993/1994 a full-scale BO-105 rotor was extensively tested with a slightly different ZFL built IBC system during two wind tunnel entries in the 40x80ft² test section at NASA Ames, as referenced in [5] and [6]. Additional flight tests are currently carried out in collaboration with EUROCOPTER Germany and the DLR Braunschweig using the same BO-105 testbed mentioned above.

Beyond its roll as hardware provider, ZFL has gathered a broad spectrum of theoretical know-how that helps to assess the potential of IBC and to weigh the imposed system complexity against the expected benefits.

There are basically two driving parameters for a hydraulic IBC system: a) the maximum pitch link loads under which the actuator can still accurately follow the commanded position, and b) the maximum piston velocity which is required to introduce the desired control amplitude at a given (higher harmonic) frequency. The reliable prediction of both the IBC introduced control loads as well as the necessary amplitudes is one focus of the theoretical activities at ZFL.

Evaluation of Experimental Data and Comparison with Calculations

Power Required and Lift-to-Drag Ratio

One question, that in some sense has initiated the interest in HHC, concerns the physical limitations of rotors operating at high tangential speed. The sharp rise of power required caused by various adverse effects such as high tip MACH number, stall onset and unbalanced lift distribution limits the efficient operation of rotary wing aircraft in the high speed regime. The idea of applying 2/rev pitch control inputs and thus redistributing the lift over the rotor disk to improve the rotor performance seemed to be the obvious solution and was subject to multiple theoretical and experimental investigations.

For the 1994 wind tunnel tests mentioned earlier, several flight conditions had been set up especially to investigate these high speed effects and estimate the possible power savings. Figure 1 shows an example of the rotor power variation versus the IBC phase angle for single harmonic 1deg 2/rev blade pitch inputs. The test condition corresponds to a high speed case at $\mu = 0.4$ which is slightly beyond the level flight capability of the production BO-105. By convention, HHC phase and amplitude are implicitly defined by the equation

$$\vartheta = \vartheta_0 + \ldots + \sum_{n=2}^{6} A_n \cos(n\Omega t - \varphi_n)\,. \qquad (1)$$

During the phase sweep, it was tried to keep the rotor thrust and moments close to constant target values derived from previous (free flight) trim calculations. The highest power reduction of about 5% results from inputs at a phase angle of slightly more than 180deg. Corresponding CAMRAD calculations are shown in the same diagram and match the test data quite well. CAMRAD tends to overpredict the effect of 2/rev IBC especially at phase angles for which power required is increased. The optimal phase, however, is captured very precisely.

Since the propulsive rotor force was not observed and (re-)trimmed (however recorded) during the wind tunnel test, it was varying within the range of -5.0% and +7.2% of the reference value. Therefore, the different test points do not strictly represent the same helicopter trim condition. A better way to assess the efficiency of IBC in this case is to consider what we shall call the effective Lift-to-Drag ratio. This parameter combines the effects of thrust, propulsive force and power changes and is defined as

$$\varepsilon = \frac{C_L}{C_D + C_P / \mu}\,. \qquad (2)$$

Any increase of this parameter indicates a general improvement of the actual rotor efficiency, implying that it offers (of course within some limits) the choice to convert the positive $\Delta\varepsilon$ into higher propulsive force (i.e. flight speed), higher lift or less power consumption.

Figure 2 shows the relative variation of the effective Lift-to-Drag ratio for the same experiment. The reference value of 6.3 can be increased by up to 8.6% for an IBC phase angle of approximately 230deg. The fact that the control phases for optimal power and optimal ε differ by some 50deg for the given data underlines the necessity to include the propulsive force as part of the efficiency criterion. CAMRAD calculations have also shown that the trimmed rotor moments have quite a significant impact on the rotor power but only a weak influence on ε. Thus, data from experiments with incomplete retrim can still be reliably assessed by means of the effective Lift-to-Drag ratio.

The wind tunnel data suggest an optimum 2/rev amplitude of approximately 1.5deg yielding a slightly higher ε than for the 1deg case.

Required Actuation Power

Obviously, the combined benefits of IBC should at least to some extent outweigh mass and power penalties imposed by the IBC system. Therefore, it is certainly desirable to keep the power consumption of the IBC hydraulics smaller than the possible rotor power savings (at least in the high speed regime).

The basic question to answer is how much mechanical power is required to introduce the desired higher harmonic blade pitch motions. Starting from the relation between actuator force and position the diagrams in fig.3 and fig.4 give some insight on how the mechanical power exchange of a single IBC actuator depends upon the operating condition. The subplot fig.3d shows the power consumed by one actuator at three different HHC frequencies and 1deg amplitude averaged over one rotor revolution. In this case at $\mu = 0.10$, the influence of the IBC phase angle on the actuator power is small. It is interesting to notice that the maximum and minimum peak values (not shown here) grow almost linearly with the control frequency, while the rise of the averaged power values is considerably slower.

As expected, the loads reach a higher level at $\mu = 0.40$, but show similar trends. One particularity, however, arises from 2/rev inputs. For phase angles between 160deg and 300deg, the power flow is reversed and the aerodynamic moments acting on the blade are feeding mechanical work into the actuator (although a small amount of less than 18W only), see figs.4d and 4e. As long as the actuators are separately servo valve controlled this feature, however, does not help saving any actuation power. Till now sizing of the hydraulic system has to be based upon the peaks of the load × speed product and would lead to roughly 4×450W = 1.8kW in this particular case (no maneuver load reserve considered, for additional data on the power consumption, see ref.[6]). These facts have inspired ZFL to extend the investigations towards highly efficient alternative hydraulic and electrical actuator designs.

Vibration

The reduction of helicopter vibrations through HHC/IBC has successfully been demonstrated in several experimental programs, ranging from MACH-scaled or full-scale wind tunnel tests (see refs.[8,9,11] and refs.[5,6], resp.), to several flight test campaigns, (e.g. refs.[3,4,12]). This section surveys some of the results with the main focus put on the question which control harmonics at what amplitudes are necessary to realize the desired vibration reduction. Note that the term vibrations in this paper refers to hub excitations by forces and moments expressed in terms of MTOW related accelerations.

The results shown in the following diagrams refer to the collaborative NASA/ZFL activities using a full scale BO-105 rotor in the 40x80ft² wind tunnel [6]. The vibrations are compared for three different free flight conditions (figs.5 to 7): level flight at $\mu = 0.10$, 5.9deg decent at $\mu = 0.10$ and 5.6deg decent at $\mu = 0.15$. The rotor thrust was trimmed to $C_T/\sigma = 0.075$ in all three cases. Figure 5a shows the basic vibrations in terms of a combined hub acceleration criterion

$$J = \frac{\hat{T} + (\hat{L} + \hat{M}) / h}{3 m_{MTOW} g} . \qquad (3)$$

The level flight at $\mu = 0.10$ clearly exhibits the strongest vibratory excitations.

To give an impression of how effectively the dominant 4/rev vibrations can be influenced by higher harmonic inputs, fig.5b shows the relative effectiveness of the different control harmonics. The values have been calculated from the acceleration amplitude changes caused by 1deg single mode inputs through geometric averaging over the complete control phase range. The diagram indicates, slightly misleading, the important roll of (b+1)/rev control for vibration reduction (comp. the morphologic scheme below). 2/rev inputs, on the other hand, show only minor effectiveness.

The next diagram contrasts the required amplitudes (equivalent to the technical effort), fig.6a, with the achievable hub vibration reduction (representing the gained benefit), fig.6b. All values represent optimal control settings (amplitude and phase) as calculated from the wind tunnel data. This principle of relating the possible benefit to the required effort is carried on through the following examples and will finally lead to the morphologic scheme as discussed in the next chapter.

While no single harmonic input ('Single Mode') is able to reduce the combined vibrations by more than 74% and usual values range from 30% to 40%, control functions of optimally chosen multiharmonic content ('Mixed Mode') were able to reduce the vibrations by at least 95% in all flight conditions considered, fig.7. The resultant half-peak-to-peak values, which depend upon the individual phase relationships, are added in fig.7a since they are essential in defining the required actuator stroke.

The lower parts of figs.6 and 7 introduce a simple way to classify effort and benefit in terms of a grade 0 to 3 ranking. The 'effort' grades directly reflect the required amplitudes:

$$\begin{aligned} 0.0 < A_n &\le 0.5\,\text{deg} \quad => \quad 1 \\ 0.5 < A_n &\le 1.0\,\text{deg} \quad => \quad 2 \\ A_n &> 1.0\,\text{deg} \quad => \quad 3. \end{aligned}$$

Merging the c and d parts of the figures into one single table one could view the pairs of grades as mathematical fractions roughly representing the efficiency of the different harmonics.

For comparison, figs.8 and 9 present similar results from earlier tests where sufficient data have been published and where the technically controllable pitch amplitude seemed to have exceeded the optimum values. Figure 8 presents single mode results from the ACTHOR program, ref [9], carried out by the DLR using a MACH-scaled 1:2.5 rotor similar to the BO-105. The blade loading was C_T/σ = 0.057 for both level flight test conditions. Pitch and roll moments had been constantly trimmed to zero. The vibration criterion combines all five rotor acceleration components (except rotor torque). 3/rev inputs proved most successful in reducing the vibrations although there is no obvious explanation why in this case reductions of the combined accelerations by 97% could be achieved with one single harmonic.

Figure 9 shows results from the OH-6A HHC flight tests conducted in 1982 by Hughes. The vibration criterion represents the vertical, longitudinal, and lateral accelerations measured at the pilot seat. The optimal amplitudes of the harmonic components calculated by the adaptive controller during the flight never exceed 0.5deg, while the resultant vibration reduction reaches approximately 85% in both level flight conditions.

In all the above cases the required amplitudes as well as the mixed mode half-peak-to-peak values stay below 2deg. Since the achievable reductions are most impressive in flight regimes with high baseline vibrations, most investigations were focused on low speed conditions. However, the results available suggest that the required amplitudes for this application do not increase considerably with speed.

Morphologic Scheme

As exemplified by figs.6c/d and 7c/d, various results gained from the broad spectrum of wind tunnel data have been condensed into one single table, the so-called morphologic scheme, fig.10. The 'effort' classification is the same as above, whereas the 'benefit' has been classified according to the corresponding goal. The verbal description would range

from not worth any effort => 0
to highly successful => 3.

The lower portion gives an even more condensed statement of both how useful the different harmonics are in general and what technical effort had to be accepted to realize these achievements. The ratio in the last line gives a crude estimate of how efficient the different harmonics finally are.

Without any further restrictions this table refers to a BO-105 type rotor only. Moreover, no multi-target optimizations have been included in the scheme, i.e. no conclusions should be drawn in this respect. As a matter of fact, the control phases for optimal results in different fields rarely coincide. Conversely, as frequently stated in the literature, the application of higher harmonic pitch control inputs optimized for one goal is likely to exhibit some negative influence on other target parameters. In some cases, however, good compromises with improvements in two or more fields have been demonstrated, see ref.[6] e.g. Based on this matrix some general conclusions can be drawn:

- The most essential harmonics are 2/ref, (b-1)/rev and b/rev.
- 2/rev inputs are highly efficient not only in improving the rotor performance but also in reducing noise. Therefore, HHC introduced from the nonrotating frame through a conventional swashplate is subject to considerable restrictions (unless $b \leq 3$).
- Only few applications are requiring control amplitudes of more than 1deg.
- Successful vibration reduction necessitates the simultaneous application of multiple control frequencies.

This morphologic scheme has already proven useful in supporting decisions on certain hardware requirements such as maximum IBC frequency and necessary actuator stroke.

Extrapolating the Results to Different Rotor Types

It is obvious that the transfer of IBC results from one type of rotor to another is subject to certain restrictions. The effects of higher frequency blade pitch control strongly depend not only on the operating condition but also on the dynamic and aerodynamic properties of the rotor. However, this section presents some straightforward analytical results which relate the extent to what the higher harmonic blade pitch inputs affect the rigid flapping, the blade root shear forces, and the local angle of attack to basic design parameters of the rotor. The underlying idea is that the positive effects of IBC originate from (at least) three distinguishable mechanisms:

A) Local alteration of the blade path. As far as the blade vortex interaction (BVI) phenomenon is concerned, the path of the relevant blade portion relative to the passing vortex is the decisive factor. Therefore, IBC can help to increase the blade vortex distance by locally steering the blade off its regular path (main application: noise).

B) Reduction of vibratory blade reactions. While aerodynamic blade moments invoke angular blade motions in the first place, shear forces are directly transferred to the hub producing undesired excitations in the nonrotating frame. IBC can be used to intentionally produce counteracting forces which cancel the basic vibrations (main application: vibration and load reduction).

C) Redistribution of the lift over the rotor disk. This approach seeks to suppress unfavorable operating conditions (stall, drag divergence, etc.) at particular portions of the rotor disk and to improve the lift efficiency with respect to the generated profile power. Especially the high speed regime offers some potential for this principle. Thus, the question in this case is, how the angle of attack can locally be modified through IBC (main application: rotor performance).

The analytical results presented here are based on the usual linearized equations assuming constant inflow, small hinge offset, and a negligible tip loss factor. Similar results can be found in refs.[1] and [2].

Figure 11a shows a BODE plot of the flapping (corresponding to *A)*, see above) and shear force (see *B)* above) response to blade pitch inputs in hover. As generally known, the effectiveness in exciting the flapping motion through harmonic blade pitch inputs decreases by 40dB/dec over the frequency. In case of the shear force, the output/input ratio first decreases and then settles at a constant value.

The corresponding diagrams on the right hand side clarify the influence of the LOCK number on the flapping response for discrete rotor harmonic frequencies. It becomes obvious that for heavier blades higher control amplitudes have to be applied to produce the same effect. This is considerably different from the conventional 1/rev control, where the β/ϑ gain is always approximately one. The gain equation given below considers the influence of the advance ratio, which, however, for reasonable values remains negligible.

$$|\beta_n / \vartheta_n| = \frac{1+\mu^2}{n\sqrt{X^2+1}} \qquad (4)$$

Although derived by harmonic balance for discrete rotor harmonic frequencies $n\Omega$ in ref [2], the same equ.(4) holds for arbitrary frequencies.

In addition to the translatory excitations, blade shear forces will also cause hub moments unless the rotor is centrally hinged. The extent to what these forces are converted into moments mainly depends on the hinge offset. This implies that the control amplitudes required to counteract similar vibratory levels in the non-rotating frame can be different according to the actual hinge offset.

Concerning the mechanism *C)* discussed above, fig.12a shows a corresponding BODE plot describing the angle of attack changes at the blade profile due to harmonic blade pitch inputs. Roughly speaking, the flapping motion tends to cancel out the blade pitch changes preventing them from fully take effect as angle of attack changes. Thus, flapping motion and angle of attack show opposite trends with respect to frequency and LOCK number (comp. figs.11b and 12b). The response at 1/rev is perfectly canceled and therefore independent of the blade weight. Yet for the typical HHC frequencies between 2/rev and 6/rev heavier blades respond with higher angle of attack changes and therefore should require smaller input amplitudes to achieve the desired effect. For $\mu = 0$, the gain is described by the equation

$$|\alpha_n / \vartheta_n| = \frac{1}{\sqrt{(1/X)-1}} \, . \qquad (5)$$

The phase shift results are considered less important, for the free choice of the IBC phase angle is not restricted by any technical limit.

The authors are aware of the fact that the relations presented here are neglecting some important effects. It is well documented that higher order elastic blade modes as well as higher frequency aerodynamic effects substantially contribute to the blade response problem. The question how efficient the blade root pitch motion can be transferred to the aerodynamically relevant outer portions can be strongly affected by the torsional dynamic properties of the blade. Similarly, the 2nd flapwise bending mode is often believed to significantly contribute to the IBC response problem, e.g. ref [8]. This means that unless two rotors are dynamically similar the theoretical extrapolation of results should be done with great care. However, it is felt that the presented analytical relations are well suited to serve as foundation for any deeper investigations.

Hardware Related Investigations

Modeling of Control Kinematics

Replacing the fixed control rods by linear actuators introduces a new degree of freedom into the control chain. New relative motions can occur which raise questions on clearance and kinematic compatibility. Therefore ZFL uses a compact algebraic method to analyze the relative displacements in the control system. The code is able to automatically generate the loop equations of arbitrary multi-linkage spatial (3D) mechanisms. It is also used to iteratively solve these equations. This process yields the geometric information necessary to confirm the proper function of the complete control system in all extreme positions.

Figure 13 shows a symbolic representation of the conventional blade control mechanism extended by an IBC actuator. For a recent application all necessary equations have been generated based on this sketch and then were evaluated for a great number of interesting positions. An impression of how the method performs is presented in fig.14. The algorithm starts the iterative search from a roughly estimated position and quickly reduces the initial error showing fast convergence.

Modeling of Actuator Dynamics

In order to generate accurate and fast blade pitch motions the feedback system which controls the actuator movements has to be optimized for the basic actuator. Therefore, the precise knowledge of the actuator dynamics and their reliable prediction helps to improve the over-all performance of the control system.

Another, safety related, aspect concerns the reduction of the control system stiffness as soon as the typically very stiff control rod is substituted by a movable element. Experiment and analysis in this field must assure that the required minimum stiffness of the complete control system does not drop below a certain critical level.

BODE plots of an actuator transfer function (actual to commanded position) are shown in fig.15. The comparison between test rig data and analysis shows excellent agreement for both investigated inner loop control gains. The linear dynamic model evaluated for this plot has been extracted from a larger generic model which accurately describes the underlying physics.

BO-105 Flight Testing

As mentioned earlier, ZFL has accumulated many hours in flight and wind tunnel testing of complete IBC systems. Building upon the experience gained during the 1990/1991 flight test campaigns, ZFL is currently participating in another flight test program. Cooperation partners are EUROCOPTER Germany and the DLR Braunschweig. This time the modified actuators enable maximum IBC amplitudes of ±1.2deg. The main focus will be placed on BVI noise reduction experiments. One goal is to validate the full-scale wind tunnel results which have shown a noise reduction of up to 6dB, ref.[6]. For more details refer to the separate paper on that subject presented at this conference.

Conclusions

During the past few years ZFL has gathered a broad spectrum of IBC related data originating from flight and wind tunnel tests, from in-house hardware testing as well as from theoretical investigations. The examples presented in this paper were chosen to relate the possible benefits to the effort in terms of required amplitudes and more specifically in terms of actuation power.

In the field of rotor performance, the effective Lift-to-Drag ratio has proven to be a useful criterion for the performance benefit. The required amplitudes for optimum results in this field should not considerably exceed 2deg even for helicopters with higher LOCK numbers than that of the BO-105. Interestingly enough, the averaged theoretical actuation power for optimal 2/rev control was found to be slightly negative pointing at the potential for a smart design of a power efficient IBC system.

As shown by many research groups vibration reduction can be realized to an impressive degree for a broad spectrum of flight conditions. Applying multi-harmonic (mixed mode) inputs, hub excitations of three or more components can simultaneously be reduced by typically over 90%. The required half-peak-to-peak values again stay below 2deg for usual helicopters.

Other benefits, although not discussed in detail in this paper, have been included in the presented morphologic scheme. Moreover, some hints on the question how to theoretically scale the results for application to different rotor types were given. They may help to estimate the possible deviations from the measured results.

The kinematic and dynamic modeling of the control system has become an important task for ZFL inasmuch as the introduction of IBC actuators in the rotating frame constitutes a significant modification of the conventional control system.

References

[1] W. Steward, **Second Harmonic Control on the Helicopter Rotor,** R.A.E. Report Aero. 2472, November 1952

[2] P.R. Payne, **Higher Harmonic Rotor Control - The Possibilities of Third and Higher Harmonic Feathering for Delaying the Stall Limit in Helicopters,** Aircraft Engineering, August 1958

[3] E.R. Wood, R.W. Powers, J.H. Cline, C.E. Hammond, **On Developing and Flight Testing a Higher Harmonic Control System,** 39th Annual Forum of the American Helicopter Society, 1983

[4] P. Richter, H.-D. Eisbrecher, V. Klöppel, **Design and First Tests of Individual Blade Control Actuators,** 16th European Rotorcraft Forum, 1990

[5] P. Richter, A. Blaas, **Full Scale Wind Tunnel Investigation of an Individual Blade Control System for the BO 105 Hingeless Rotor,** 19th European Rotorcraft Forum, 1993

[6] S. A. Jacklin, A. Blaas, S. M. Swanson, D. Teves, **Second Test of a Helicopter Individual Blade Control System in the NASA Ames 40- By 80-Foot Wind Tunnel,** 2nd AHS International Aeromechanics Specialists' Conference, 1995

[7] G. Reichert, **Helicopter Vibration Control - A Survey,** Sixth European Rotorcraft and Powered-Lift Aircraft Forum, 1980

[8] G. Lehmann, **Untersuchungen zur höherharmonischen Rotorblattsteuerung bei Hubschraubern,** Ph.D. Thesis, Institute of Flight Mechanics, Technical University Braunschweig, 1987

[9] R. Kube, G. Lehmann, S. Malke, **Ergebnisse der HHC-Windkanalversuche 1986/88,** DLR-Report IB III-89/25, Deutsche Forschungsanstalt für Luft- und Raumfahrt, Braunschweig, 1989

[10] A. Blaas, J. Götte, W. Pflüger, **IBC-Windkanalversuche 1993 - 1994,** ZFL-Report IBC-393-1295, Kassel, 1995

[11] C.E. Hammond, **Wind Tunnel Results Showing Rotor Vibratory Loads Reduction Using Higher Harmonic Blade Pitch,** 36th Annual Forum of the American Helicopter Society, Washington D.C., 1980

[12] M. Polychroniadis, M. Achache, **Higher Harmonic Control: Flight Tests of an Experimental System on SA 349 Research Gazelle,** 42nd Annual Forum of the American Helicopter Society, Washington D.C., 1986

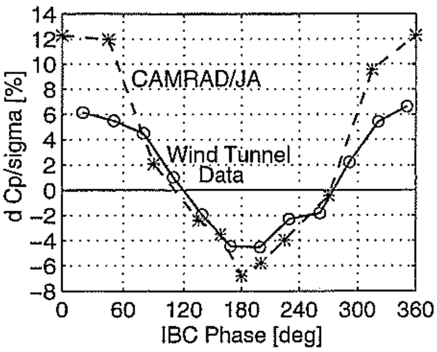

Figure 1: Rotor Power Required Changes due to 1deg 2/rev Inputs versus Control Phase Angle, Comparison of Wind Tunnel Data with CAMRAD Calculations (Propulsive Force not Trimmed)

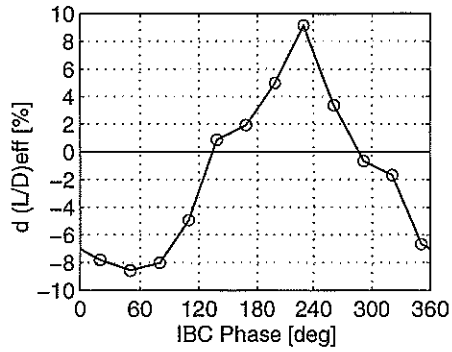

Figure 2: Impact of 1deg 2/rev Inputs on Effective Lift-to-Drag Ratio Calculated from Wind Tunnel Data (Propulsive Force not Trimmed)

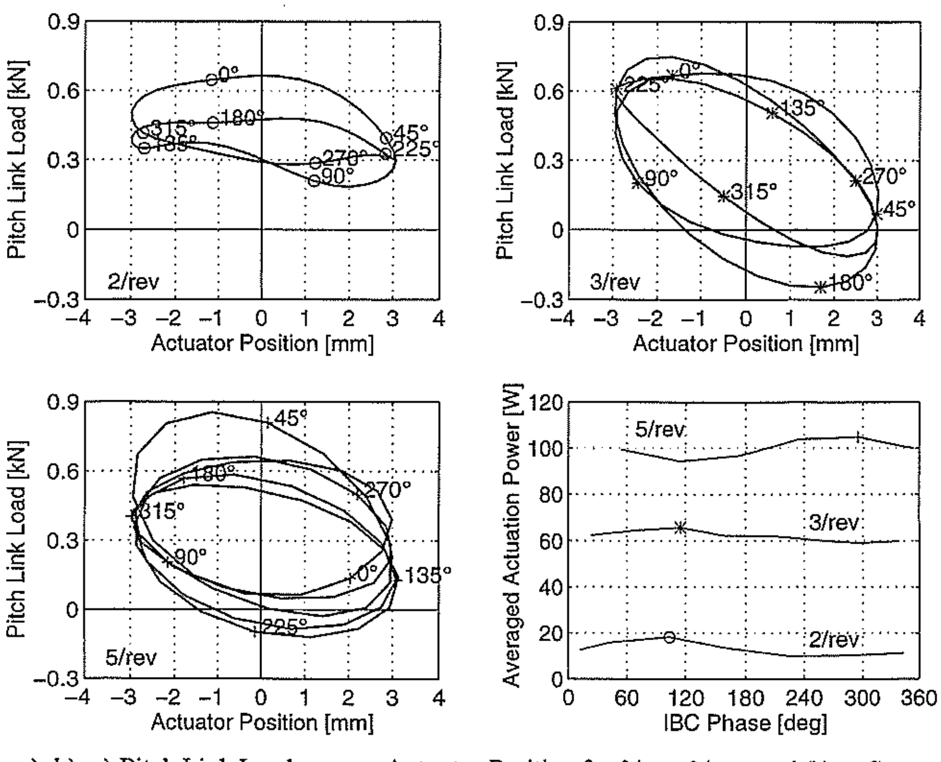

Figure 3: a), b), c) Pitch Link Loads versus Actuator Position for 2/rev, 3/rev, and 5/rev Control (1deg)
d) Averaged Theoretical Actuation Power versus Control Phase Angle

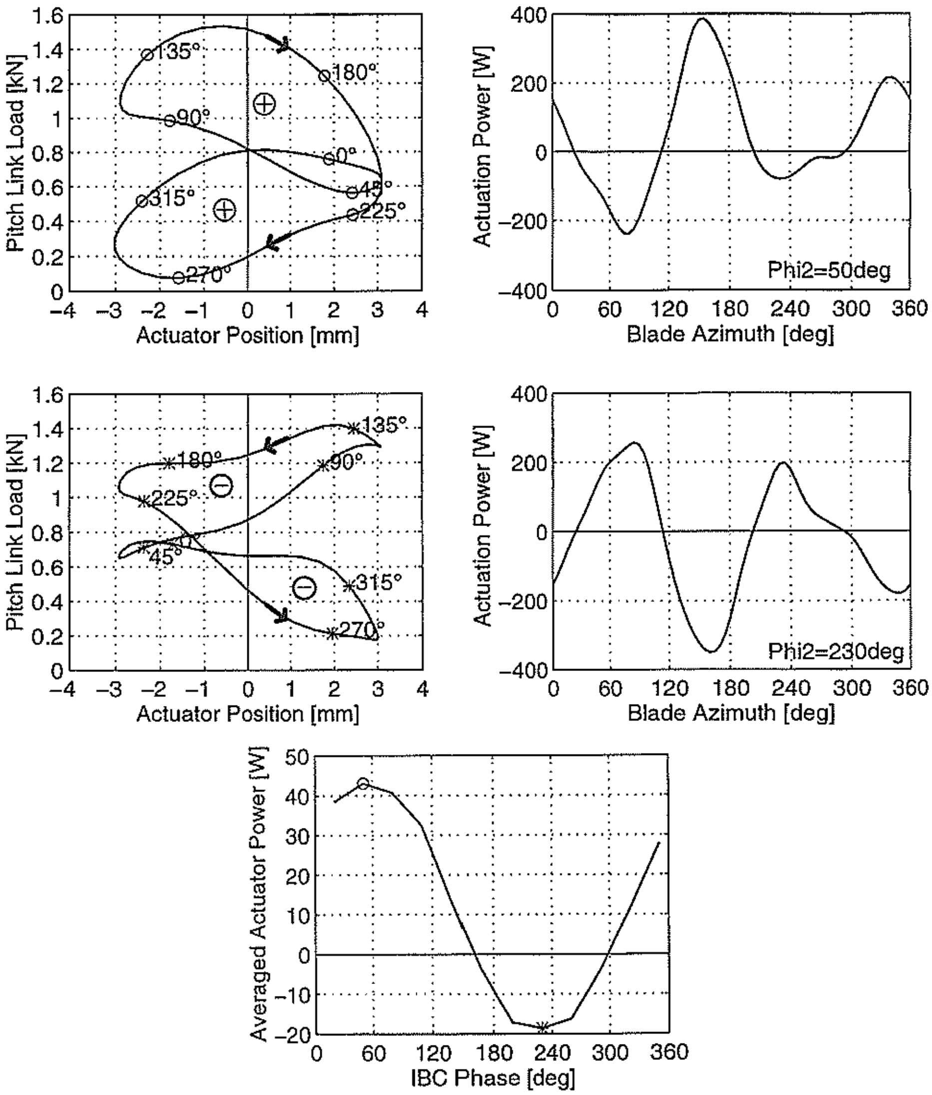

Figure 4: a), c) Pitch Link Loads vs Actuator Position for 2/rev Inputs at Two Selected Control Phase Angles
b), d) Corresponding Theoretical Actuation Power for One Actuator versus Blade Azimuth Angle
e) Averaged Theoretical Actuation Power versus Control Phase Angle

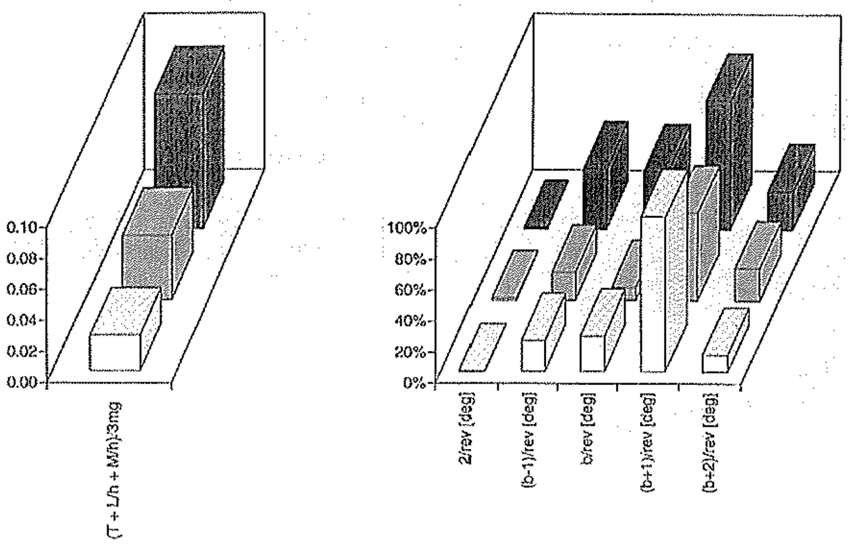

Figure 5: a) Baseline 4/rev Hub Accelerations for Three Operating Conditions (BO-105 Wind Tunnel Data)
b) Sensitivity of 4/rev Accelerations to Single-Harmonic Control Inputs

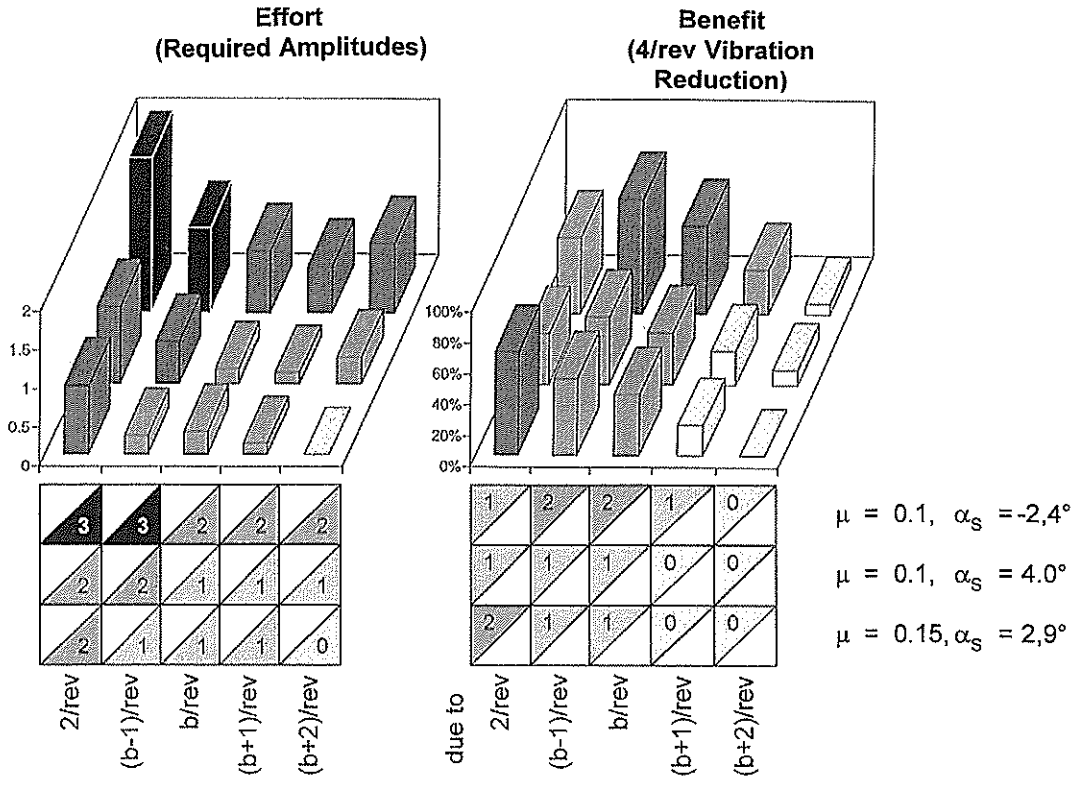

Figure 6: a) Calculated Optimal Single Mode Control Amplitudes (BO-105 Wind Tunnel Data)
b) Corresponding Reduction of 4/rev Hub Accelerations
c), d) Classification of 'Effort' as shown in a) and 'Benefit' as shown in b)

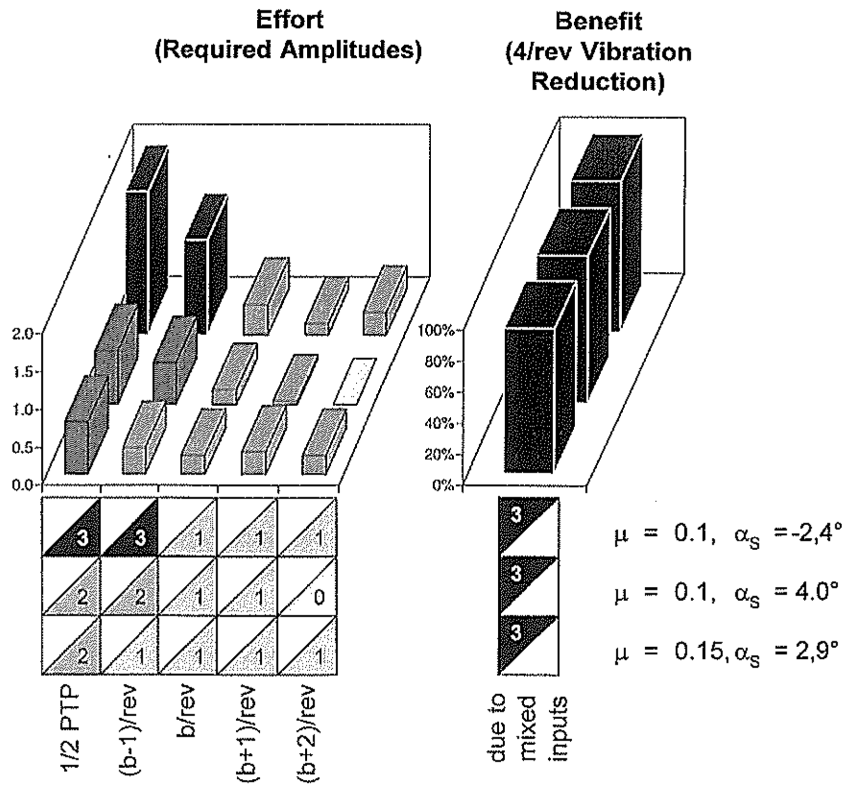

Figure 7: a) Calculated Optimal Mixed Mode Control Amplitudes (BO-105 Wind Tunnel Data)
b) Corresponding Reduction of 4/rev Hub Accelerations
c), d) Classification of 'Effort' as shown in a) and 'Benefit' as shown in b)

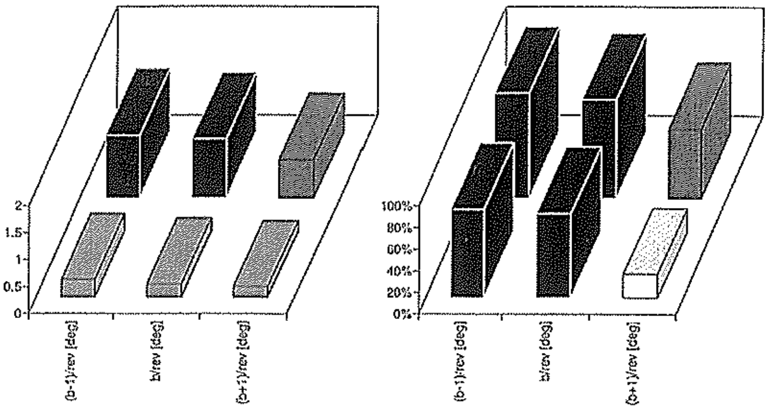

Figure 8: a) Optimal Single Mode Control Amplitudes (ACTHOR Wind Tunnel Experiments, Ref.[9])
b) Corresponding Reduction of 4/rev Hub Accelerations

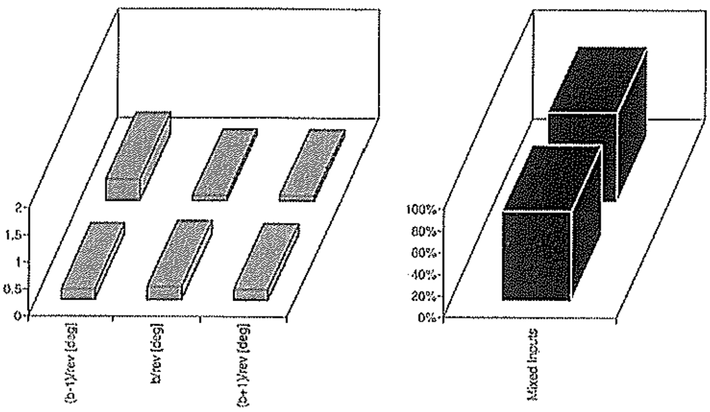

Figure 9: a) Optimal Mixed Mode Control Amplitudes (Hughes OH-6A Flight Tests, Ref.[3])
b) Corresponding Reduction of 4/rev Accelerations at Pilot Seat

Goal	Flight Condition	2/rev	(b-1)/rev	b/rev	(b+1)/rev	(b+2)/rev	Mixed Mode
Noise Reduction	μ = 0.1, α_S = +4.0°	2 / 3	3 / 2	1 / 1	0 / 2	0 / 1	3 / 3
	μ = 0.15, α_S = +2,9°	1 / 2	1 / 1	2 / 2	2 / 2	0 / 2	2 / 3
Vibration Reduction	μ = 0.1, α_S = - 2.4°	1 / 3	2 / 3	2 / 2	1 / 2	0 / 2	3 / 3
	μ = 0.1, α_S = +4.0°	1 / 2	1 / 2	1 / 1	0 / 1	0 / 1	3 / 2
	μ = 0.15, α_S = +2,9°	2 / 2	1 / 1	1 / 1	0 / 1	0 / 0	3 / 2
Performance Improvement	$\mu \geq 0.3$	3 / 2	2 / 2	0 / 2	- / -	- / -	- / -
Blade Load Reduction		2 / 2	0 / 0	1 / 1	0 / 1	0 / 1	- / -
Pitch Link Load Reduction		2 / 1	1 / 1	1 / 1	1 / 1	1 / 1	- / -
Unweighted Average / Maximum Value		1.8 / 3	1.4 / 3	1.1 / 2	0.6 / 2	0.1 / 2	2.8 / 3
Ratio		0.6	0.5	0.6	0.3	0.1	0.9

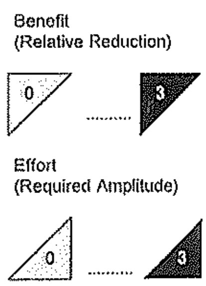

Figure 10: Morphologic Scheme: Overview of Categorized 'Effort' and 'Benefit' for Different IBC Goals

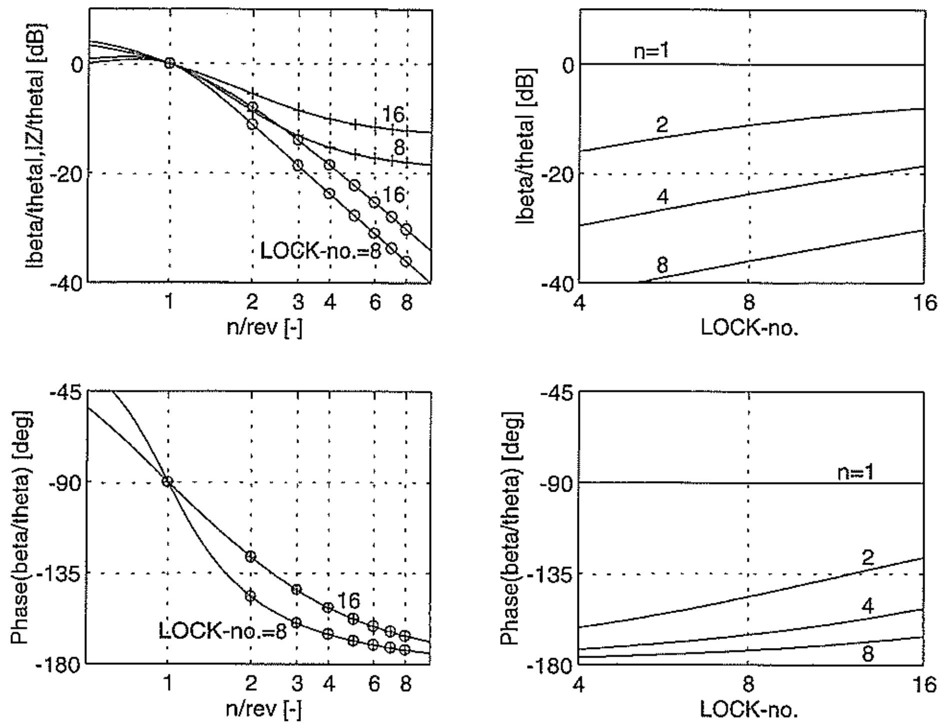

Figure 11: Flapping Angle and Blade Root Shear Force Response to Higher Harmonic Blade Pitch Control:
a) BODE Plot; b) Effect of LOCK Number

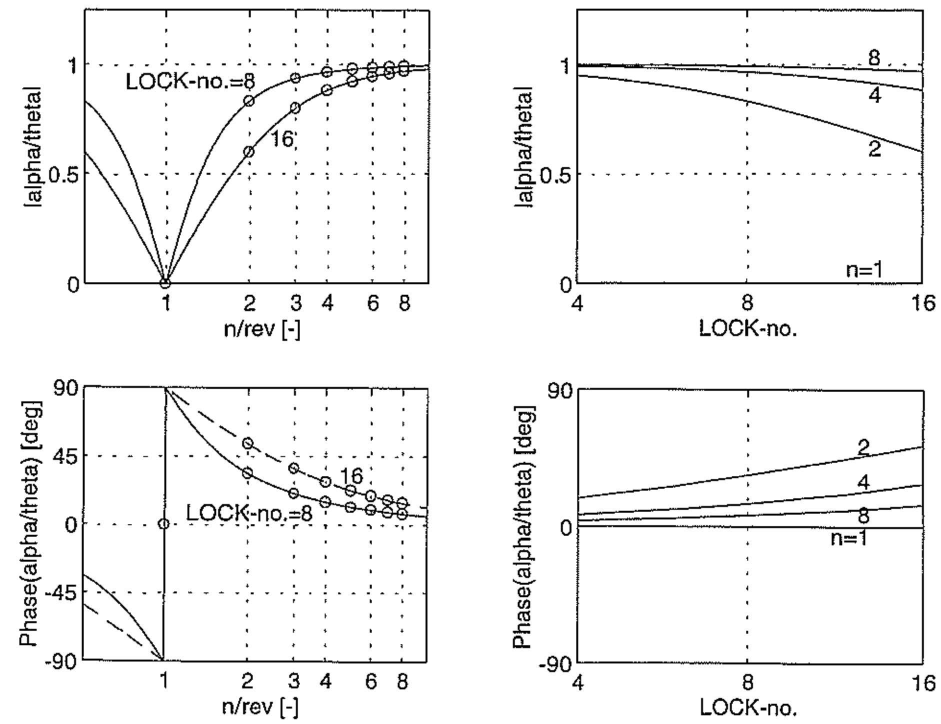

Figure 12: Blade Profile Angle of Attack Change due to Higher Harmonic Blade Pitch Control:
a) BODE Plot; b) Effect of LOCK Number

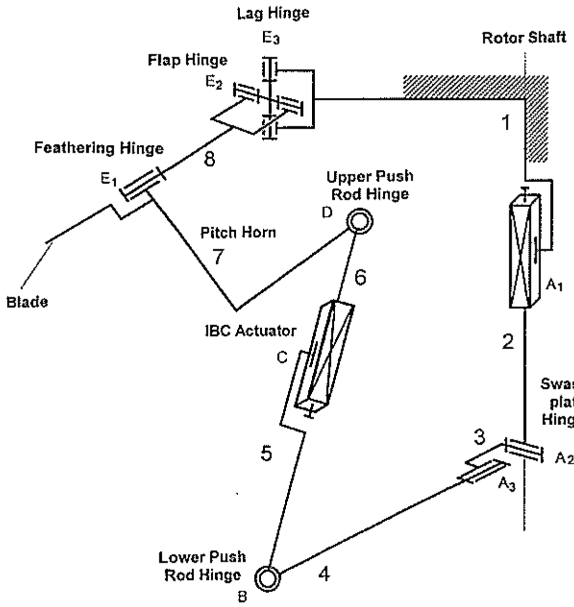

Figure 13: Spatial Kinematic Setup of Blade Pitch Control System with IBC Actuator, Hinge and Linkage Definitions

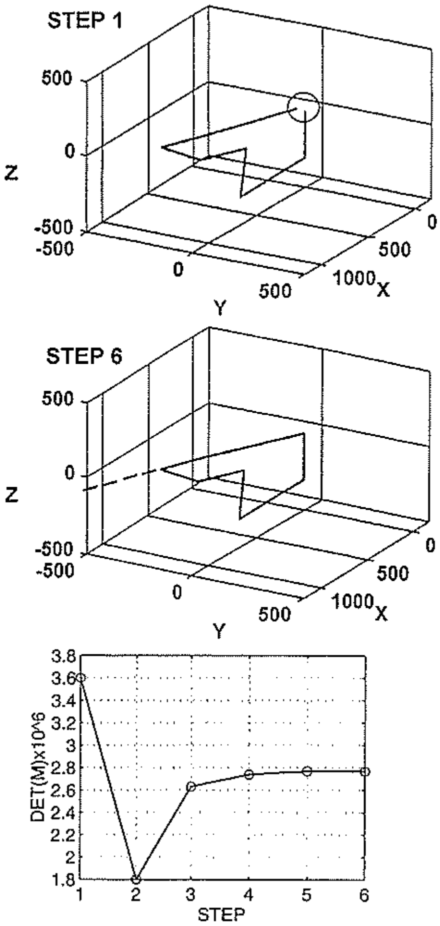

Figure 14: Performance of ZFL Kinematic Solver:
a), b) 3D Control Element Positions
c) Numerical Convergence

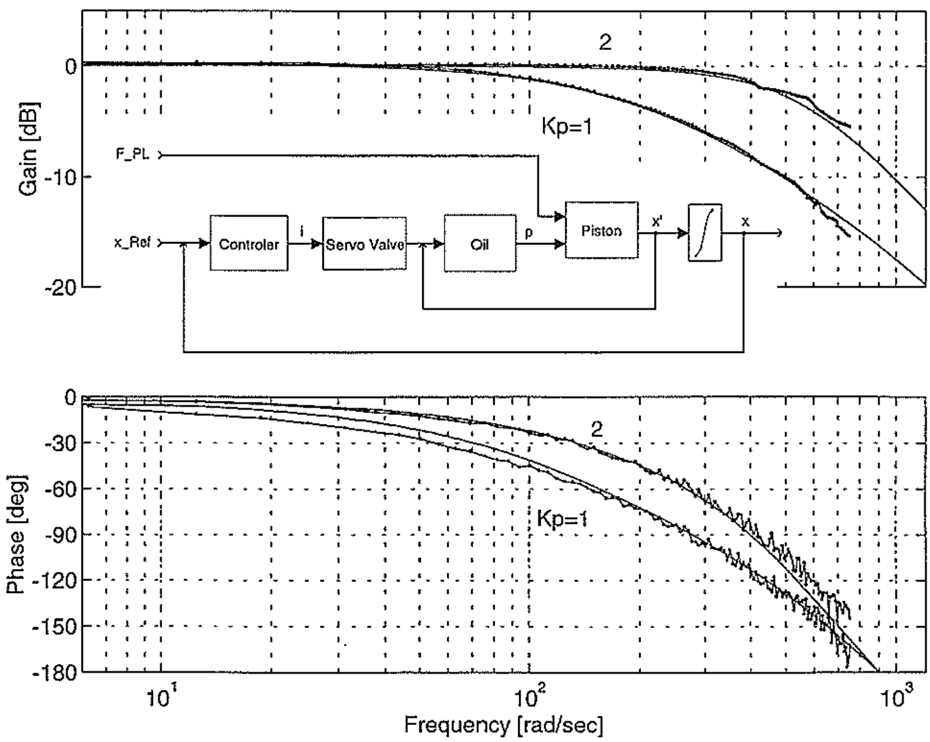

Figure 15: IBC Actuator Dynamic Modeling:
a) BODE Plot of Actual to Commanded Position Response, Measurements versus Model Results
b) Signal Block Diagram